Fracture of model end-linked networks

Christopher W. Barney[a,1,2], Ziyu Ye[b,1,3], Ipek Sacligil[a,1], Kelly R. McLeod[a], Han Zhang[c], Gregory N. Tew[a,4], Robert A. Riggleman[c,4], and Alfred J. Crosby[a,4]

[a]Polymer Science and Engineering Department, University of Massachusetts Amherst, Amherst, MA 01003; [b]Department of Chemistry, University of Pennsylvania, Philadelphia, PA 19104; and [c]Department of Chemical and Biomolecular Engineering, University of Pennsylvania, Philadelphia, PA 19104

Edited by David Weitz, Department of Physics, Division of Engineering and Applied Science, Harvard University, Cambridge, MA; received July 12, 2021; accepted January 8, 2022

Advances in polymer chemistry over the last decade have enabled the synthesis of molecularly precise polymer networks that exhibit homogeneous structure. These precise polymer gels create the opportunity to establish true multiscale, molecular to macroscopic, relationships that define their elastic and failure properties. In this work, a theory of network fracture that accounts for loop defects is developed by drawing on recent advances in network elasticity. This loop-modified Lake–Thomas theory is tested against both molecular dynamics (MD) simulations and experimental fracture measurements on model gels, and good agreement between theory, which does not use an enhancement factor, and measurement is observed. Insight into the local and global contributions to energy dissipated during network failure and their relation to the bond dissociation energy is also provided. These findings enable a priori estimates of fracture energy in swollen gels where chain scission becomes an important failure mechanism.

chain scission | loop defects | Lake–Thomas theory | gel mechanics

Models that link materials structure to macroscopic behavior can account for multiple levels of molecular structure. For example, the statistical, affine deformation model connects the elastic modulus E to the molecular structure of a polymer chain,

$$E_{aff} = 3\nu k_b T \left(\frac{\phi_o^{\frac{1}{3}} R_o}{\phi^{\frac{1}{3}} R} \right)^2, \quad [1]$$

where ν is density of chains, ϕ is polymer volume fraction, R is end-to-end distance, ϕ_o and R_o represent the parameters taken in the reference state that is assumed to be the reaction concentration in this work, and $k_b T$ is the available thermal energy where k_b is Boltzmann's constant and T is temperature (1–6). Refinements to this model that account for network-level structure, such as the presence of trapped entanglements or number of connections per junction, have been developed (7–11). Further refinements to the theory of network elasticity have been developed to account for dynamic processes such as chain relaxation and solvent transport (12–17). Together these refinements link network elasticity to chain-level molecular structure, network-level structure, and the dynamic processes that occur at both size scales.

While elasticity has been connected to multiple levels of molecular structure, models for network fracture have not developed to a similar extent. The fracture energy G_c typically relies upon the large strain deformation behavior of polymer networks, making it experimentally difficult to separate the elastic energy released upon fracture from that dissipated through dynamic processes (18–26). In fact, most fracture theories have been developed at the continuum scale and have focused on modeling dynamic dissipation processes (27). An exception to this is the theory of Lake and Thomas that connects the elastic energy released during chain scission to chain-level structure,

$$G_{c,LT} = \frac{\text{Chains}}{\text{Area}} \times \frac{\text{Energy Dissipated}}{\text{Chain}} = \nu R_o N U, \quad [2]$$

where NU is the total energy released when a chain ruptures in which N represents the number of monomer segments in the chain and U the energy released per monomer (26).

While this model was first introduced in 1967, experimental attempts to verify Lake–Thomas theory as an explicit model, as summarized in *SI Appendix*, have been unsuccessful. Ahagon and Gent (28) and Gent and Tobias (29) attempted to do this on highly swollen networks at elevated temperature but found that, while the scalings from Eq. **2** work well, an enhancement factor was necessary to observe agreement between theory and experiment. This led many researchers to conclude that Lake–Thomas theory worked only as a scaling argument. In 2008, Sakai et al. (30) introduced a series of end-linked tetrafunctional, star-like poly(ethylene glycol) (PEG) gels. Scattering measurements indicated a lack of nanoscale heterogeneities that are characteristic of most polymer networks (30–32). Fracture measurements on these well-defined networks were performed and it was again observed that an enhancement factor was necessary to realize explicit agreement between experiment and theory (33). Arora et al. (34) recently attempted to address this discrepancy by accounting for loop defects; however, different assumptions were used when inputting U to calculate Lake–Thomas theory

Significance

Fracture of polymer networks is molecular in nature as chains must rupture for a crack to propagate. Predicting macroscopically measured fracture properties from molecular parameters a priori has remained elusive, even for well-defined networks. This work shows that a newly developed theory, which accounts for network defects, quantitatively describes both experimental measurements and molecular dynamics (MD) simulation data for fracture of a polymer network with independently defined or measured parameters. This advance provides a missing link between chemistry and materials science and engineering for polymer networks.

Author contributions: C.W.B., Z.Y., I.S., G.N.T., R.A.R., and A.J.C. designed research; C.W.B., Z.Y., I.S., and K.R.M. performed research; G.N.T., R.A.R., and A.J.C. contributed new reagents/analytic tools; C.W.B., Z.Y., I.S., K.R.M., and H.Z. analyzed data; and C.W.B., Z.Y., I.S., G.N.T., R.A.R., and A.J.C. wrote the paper.

The authors declare no competing interest.

This article is a PNAS Direct Submission.

[1]C.W.B., Z.Y., and I.S. contributed equally to this work.

[2]Present address: Materials Research Laboratory, Department of Mechanical Engineering, and Department of Chemical Engineering, University of California, Santa Barbara, CA 93106.

[3]Present address: Department of Chemical and Biomolecular Engineering, University of Delaware, Newark, DE 19716.

[4]To whom correspondence may be addressed. Email: tew@mail.pse.umass.edu, rrig@seas.upenn.edu, or acrosby@umass.edu.

This article contains supporting information online at https://www.pnas.org/lookup/suppl/doi:10.1073/pnas.2112389119/-/DCSupplemental.

Published February 10, 2022.

values that again required the use of an enhancement factor to achieve quantitative agreement. In this work we demonstrate that refining the Lake–Thomas theory to account for loop defects while using the full bond dissociation energy to represent U yields excellent agreement between the theory and both simulation and experimental data without the use of any adjustable parameters.

PEG gels synthesized via telechelic end-linking reactions create the opportunity to build upon previous theory to establish true multiscale, molecular to macroscopic relationships that define the fracture response of polymer networks. This paper combines pure shear notch tests, molecular dynamics (MD) simulations, and theory to quantitatively extend the concept of network fracture without the use of an enhancement factor. First, the control of molecular-level structure in end-linked gel systems is discussed. Then, the choice of molecular parameters used to estimate chain- and network-level properties is discussed. Experimental and MD simulation methods used when fracturing model end-linked networks are then presented. A theory of network fracture that accounts for loop defects is developed, in the context of other such models that have emerged recently, and tested against data from experiments and MD simulations. Finally, a discussion of the local and global energy dissipated during failure of the network is presented.

Synthesis of PEG Gels

Over the last decade, synthetic methods have improved the ability to prepare networks with fewer defects; specifically, end-linked networks have attracted renewed interest (11, 30, 35–38). Highly resilient networks were reported in 2012 by Crosby, Tew, and coworkers (31, 36, 39) utilizing the thiol addition across norbornene click reaction. This resilience was consistent with homogeneous networks free of nanoscale differences in cross-link density, which was later confirmed by neutron-scattering studies. The same $A_2 + B_4$ synthetic route to PEG-containing networks was used in this work and is shown in Fig. 1*A*. This well-controlled chemistry results in homogeneous networks where the mechanical properties can be easily tuned by the intentional inclusion of defects. Kawamoto et al. (40) quantified the number of dangling ends in PEG networks cross-linked by azide-alkyne click reactions, and it was observed that stoichiometric ratios of cross-linker to functionalized chains resulted in dangling ends on less than 1% of network junctions. This result shows that defects in the network of end-linked gels formed with highly efficient cross-linking reactions, such as the thiol-ene click reactions used in this study, are primarily loop defects. The characterization of network elasticity through the equilibrium swelling ratios and moduli (measured via indentation) for PEG networks swollen to equilibrium in water is shown in Fig. 1*B*. The previously established relationship between network elasticity and loop defects (11) indicates good control over loop formation with respect to ϕ. Full experimental details are contained in *SI Appendix*.

Structure of PEG Gels

PEG gels were chosen for this study to minimize losses that would increase the fracture energy. Their high solvent content reduces the impact of deformation rate and temperature on energy dissipation. In addition, the homogeneous network structure of these gels minimizes stress concentration points, which create a heterogeneous distribution of stress in front of a crack tip and increase the energy dissipated (31).

The chain-level molecular structure of gels is characterized by ν, R_o, and NU. ν can be calculated from polymer volume fraction $\phi_o = \{0.043, 0.053, 0.065, 0.083\}$, Avogadro's number, and density of PEG $\rho = 1{,}110$ kg/m^3 (41). The end-to-end distance R_o of a chain can be estimated with the Kuhn length $b = 0.72$ nm, reference volume $V_{ref} = 0.1$ nm^3, monomer volume $V_{PEG} = 0.069$ nm^3, and the input degrees of polymerization $N = \{91, 182, 273\}$ as shown in *SI Appendix* (36, 39, 42). NU can be estimated from N and the number of bonds in each monomer. Each chemical PEG monomer has three backbone bonds. From the C-C bond dissociation energy (BDE) of 334.7 kJ/mol, $U = 1.6 \times 10^{-18}$ J per monomer segment (39). Using the lower BDE for C-O gives $U = 1.4 \times 10^{-18}$ J per monomer, which is a negligible difference (33).

In addition to chain-level structure, accounting for network structure, described by the fraction of loop defects, requires an estimation of network-level features. Kawamoto et al. (40) were able to experimentally quantify loop density and used this measurement to verify that MD simulations of network formation

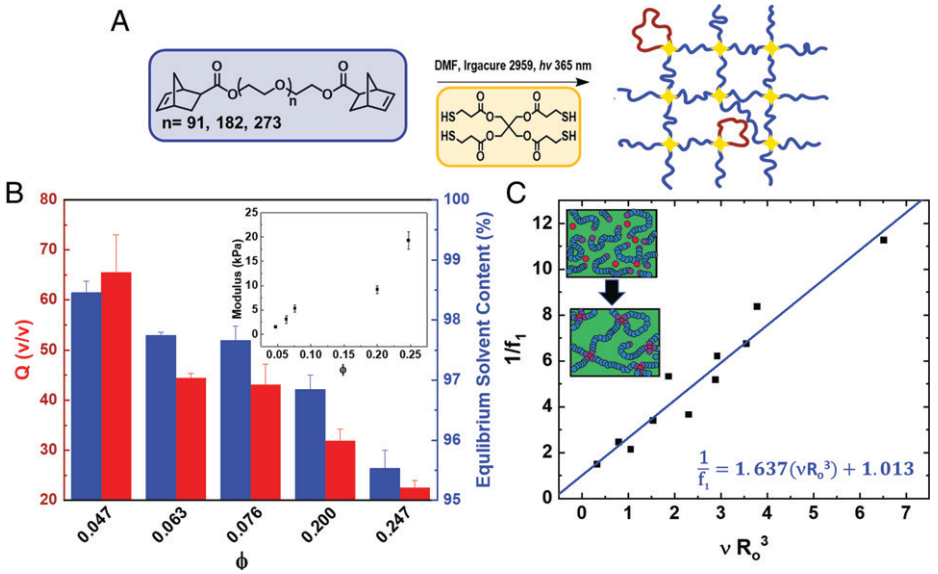

Fig. 1. (*A*) Reaction scheme for telechelic PEG network formation used in this study. The scheme shows an example network with loop defects (red) where the norbornene-functionalized PEG macromonomer and tetrafunctional thiol cross-linker are shown in blue and yellow, respectively. (*B*) Equilibrium swelling ratio Q and solvent content against initial polymer volume fraction ϕ for a series of PEG gels swollen to equilibrium in water. *Inset* shows E measured via indentation against ϕ for PEG gels in the equilibrium swollen state. (*C*) Plot showing the fraction of primary loops in the network f_1 is inversely proportional to $\nu R_o{}^3$, taken from the simulated networks.

were able to predict loop density. Building upon these findings, MD simulations were performed in this work to estimate the loop fraction for different molecular weights and concentrations. End-linked networks formed via in silico cross-linking naturally incorporate loop defects into the network structure, with the fraction of loops dictated by the initial formation condition. The number of loops were then counted by tracking polymer chains that have both functionalized end groups bonded to the same cross-linking junction. Fig. 1*C* shows that the fraction of primary loops in the network f_1 is inversely proportional to $\nu {R_o}^3$. This dependence implies that f_1 can be tuned by altering either the input chain length or initial polymer volume fraction ϕ_o (11). Secondary and tertiary loop fractions, f_2 and f_3, can be estimated assuming $f_2 = f_3 \approx 0.75 f_1$ as was found by Zhong et al. (11) for tetrafunctional networks. The effective network junction functionality F_{eff} can then be estimated as

$$\frac{F_{eff}-2}{F_{eff}} = \frac{1}{2}\left(1 - \frac{4}{3}f_1 - \frac{3}{8}f_2 - \frac{81}{4{,}961}f_3\right), \qquad [3]$$

where the right side of Eq. **3** is the correction factor proposed by Zhong et al. (11) for a tetrafunctional network with loop defects. F_{eff} is a number that is less than or equal to the chemical junction functionality F (maximum [max] number of chains connected to a cross-linking junction) and greater than 2 to remain a network. F_{eff} can then be used in the phantom model correction to the chain length to calculate an effective chain length,

$$N_{eff} = N\frac{F_{eff}}{F_{eff}-2}. \qquad [4]$$

Fracture of Simulated Networks

Simulated networks are made up of Kremer–Grest-style bead-spring polymers (43) connected by breakable quartic bonds (44) embedded in a Lennard-Jones solvent. Networks involving end-reactive polymers and tetrafunctional cross-links are prepared by explicitly simulating a cross-linking process so that the resulting networks have a realistic concentration of defects. Full details on the methods used to create and characterize simulated networks are contained in *SI Appendix*. The input BDE is defined by the energy difference between the minimum of the quartic bond potential and the local maximum that the bond energy reaches at the moment of chain scission. To induce fracture in the network, the simulation box was expanded uniaxially while constant pressure was maintained in the transverse directions until all bonds lying along a plane were ruptured (Fig. 2*A*). Cracks are difficult to define on molecular size scales and thus no initial crack was prescribed, and rupture of the chains in the simulation box was taken to be representative of failure in the cohesive zone in front of a crack tip. During deformation, the system stress was tracked as a function of the applied strain. This stress response is plotted against the engineering strain in Fig. 2*B* for both loading and unloading of the networks at different maximum strains ε_{max} (Fig. 2*C*). The total system energy dissipated due to chain scission U_{dissip} was taken as the difference in the areas under the simulated stress–strain curve from the uniaxial loading and unloading of the network at varying ε_{max},

$$U_{dissip}(\varepsilon_{max}) = V\left(\int_0^{\varepsilon_{max}} \sigma\, d\varepsilon + \int_{\varepsilon_{max}}^{0} \sigma\, d\varepsilon\right), \qquad [5]$$

as shown by the shaded region in Fig. 2 *B*, *Inset*.

The slope of the normalized energy dissipated U_{dissip}/N_{eff} vs. total number of broken chains at the corresponding breaking strains ε_{max} (Fig. 2*C*) gives the energy released per chain during fracture due to chain scission. G_c is determined from this simulated energy dissipated per chain in combination with ν and R_o.

Choosing an Estimate for *U*

In this work U is calculated from the BDE of the backbone bonds, which is a practice that has recently been called into question (45). Wang et al. (45) challenged this practice by assuming the maximum force a polymer chain could withstand and calculating the elastic energy that a single chain would contain at that point. This approach suggested that the BDE may overestimate U by a factor of ~6 (45). As discussed in *SI Appendix*, similar reasoning also led Arora et al. (34) to use a value of U that was significantly less than the BDE.

In our approach, MD simulations were used to test whether setting U to be equal to the BDE is reasonable. U_{dissip}/N_{eff} during cyclic rupture tests is plotted against the number of broken chains in Fig. 2*C*. There appears to be a weak dependence on N; however, the slope of all three chain lengths is well approximated by a single slope U_{sim} that gives the elastic energy dissipated per broken bond. The average U_{sim} value measured from all network systems at different ϕ_o and N is 89.4, which is of the same order as the value of 72.4 from the bond energy potential used in the simulations. We note that the energy of the bond when the force is a maximum is ~20 and any force-coupled reduction in the energy barrier should naturally arise from our simulations, which has been seen in simulations of other activated processes (46, 47). This result suggests that estimating U as being the same

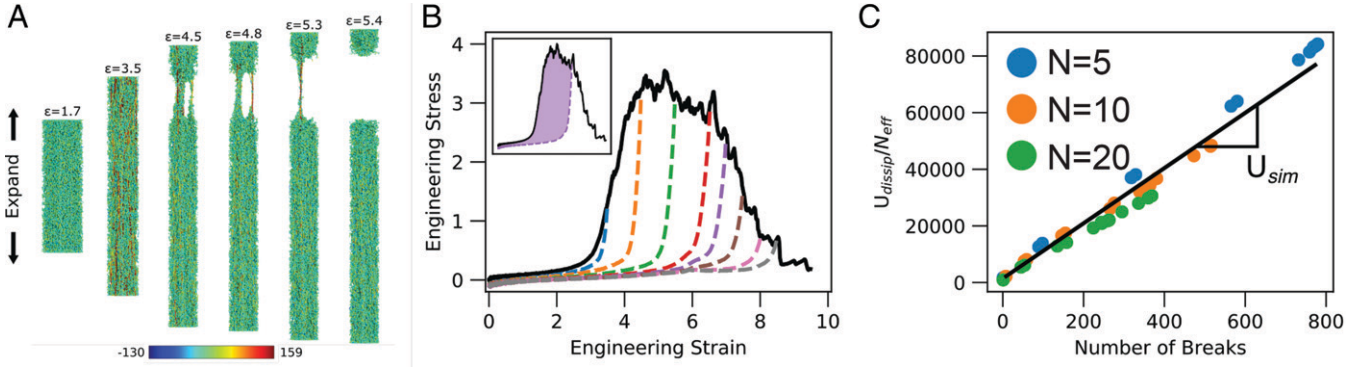

Fig. 2. (*A*) Visualization at progressively increasing engineering strain ε of a simulated fracture event in end-linked polymer network formed at $\phi_o = 0.5$ and $N = 10$. Monomer units are colored by the values of per monomer stress as shown by the color bar. (*B*) Engineering stress vs. engineering strain response for an example loading (solid line) and unloading (dashed line) process ($\phi_o = 1.0$, $N = 10$). *Inset* shows the shaded area (purple) representing the difference in energy dissipated between the loading and unloading process for a given breaking strain. (*C*) Total system energy dissipated normalized by the effective chain length (U_{dissip}/N_{eff}) as a function of the total number of chains broken at different system strains during fracture for networks formed at $\phi_o = 1.0$ and $N = \{5, 10, 20\}$. The solid line indicates the average slope of normalized energy dissipated vs. number of chains broken for networks formed at $N = \{5, 10, 20\}$.

order of magnitude as the bond dissociation energy is reasonable and will thus be the value employed for all the calculations presented in the following section. Rationalizing this difference from the arguments of Wang et al. (45) and understanding the weak residual dependence on N remain outstanding questions.

Comparison to Models

The material properties, E and G_c, should be defined by the network structure through Eqs. **1** and **2**, respectively. As shown in Fig. 3, this is not the case for both the MD simulations and experimental values. E measurements display a trend where the affine deformation model consistently overestimates experimental values. Note that G_c is measured from monotonic loading in a pure shear geometry as described in *SI Appendix*. Lin et al. (48) have recently shown that the observed fracture energy from monotonic loading of similar gels agrees with the threshold energy measured during cyclic loading. G_c measurements display a trend where the classic Lake–Thomas theory underestimates the experimental measurements. This trend is consistent with previous observations and is often attributed to an underestimation of the size scale of dissipation, which many compensate for with an enhancement factor (33, 34).

To address the mismatch in predicting E, the affine deformation model is often modified to soften the constraints of affine deformation such that junctions can fluctuate about average positions that deform affinely. These constraints are typically conceptualized as "phantom" chains constraining the real chains (49, 50). Zhong et al. (11) recently proposed a molecular model called real elastic network theory (RENT) that is capable of predicting E in networks with loop defects. RENT was developed by modifying the phantom network model to further weaken the constraints on the polymer chain in a manner consistent with loop defects. RENT assumes both that Gaussian chain statistics are valid and that the network junctions on average deform affinely with the macroscopic deformation of the sample (10) and estimates the modulus as

$$E_{RENT} = 3\nu k_b T \left(\frac{\phi_o^{\frac{1}{3}} R_o}{\phi^{\frac{1}{3}} R} \right)^2 \left(\frac{F_{eff} - 2}{F_{eff}} \right). \quad [6]$$

The RENT expression for the modulus (Eq. **6**) differs from the form presented by Zhong et al. (11) in that the loop correction creates an effective network junction functionality F_{eff}. As discussed above, F_{eff} is calculated in a manner that is consistent with the protocol outlined by Zhong et al. (11). When F_{eff} is equal to the chemical network junction functionality, $F = 4$, Eq. **6** collapses to the phantom network model. This reformulation highlights that RENT can be conceptualized as a correction for the number of elastically effective connections at network junctions. The plots of simulation and experimental measurements of E against values from RENT theory E_{RENT} in Fig. 4 show good agreement with the model once the influence of loops is included.

Building on RENT's method of accounting for loop defects when connecting E to network structure, we developed a loop-modified form of Lake–Thomas theory, which we refer to as $G_{c,RENT}$, that increases the size scale of dissipation based on the underlying physics of polymer networks,

$$G_{c,RENT} = \nu_{eff} R_{eff} N_{eff} U = \nu R_o N U \left(\frac{F_{eff}}{F_{eff} - 2} \right)^{\frac{1}{2}}. \quad [7]$$

This model suggests that the fracture energy includes a contribution from the energy released in the network surrounding the

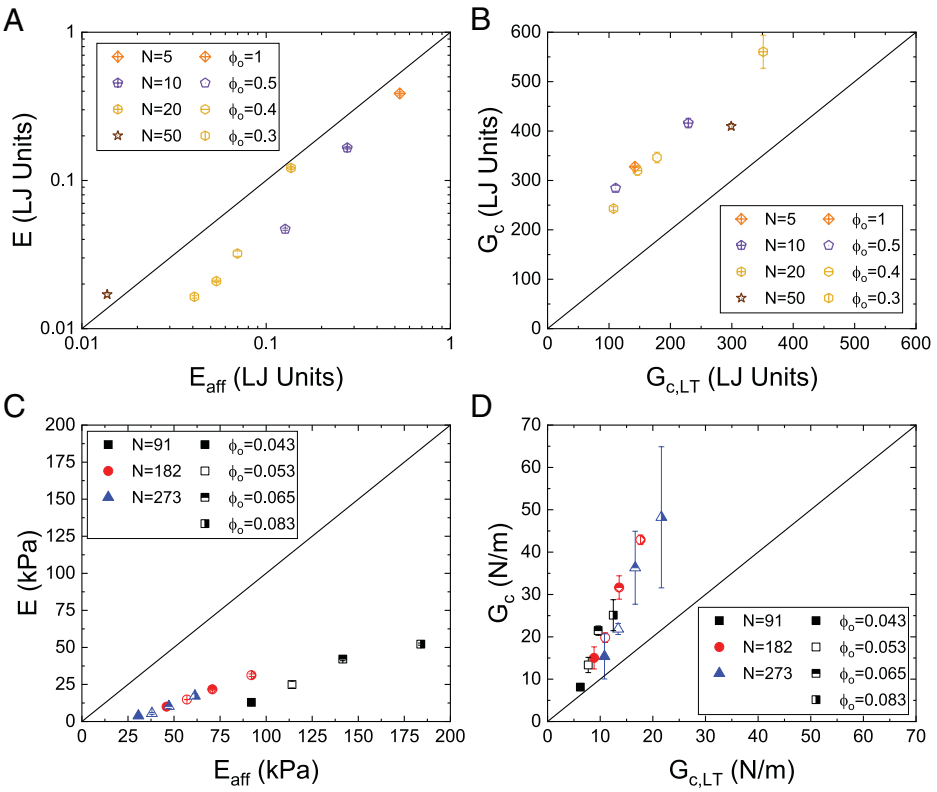

Fig. 3. Plot of E and G_c measured via (*A* and *B*) MD simulations and (*C* and *D*) indentation and notch tests, described fully in *SI Appendix*, performed on a series of PEG gels in the as-prepared state (no additional swelling step) against estimates calculated from the classic statistical affine deformation model and Lake–Thomas theory, respectively. MD simulation values are given in reduced Lennard-Jones (LJ) units. The black line represents the equivalent point. The theory consistently overestimates the observed values of E and underestimates those for G_c.

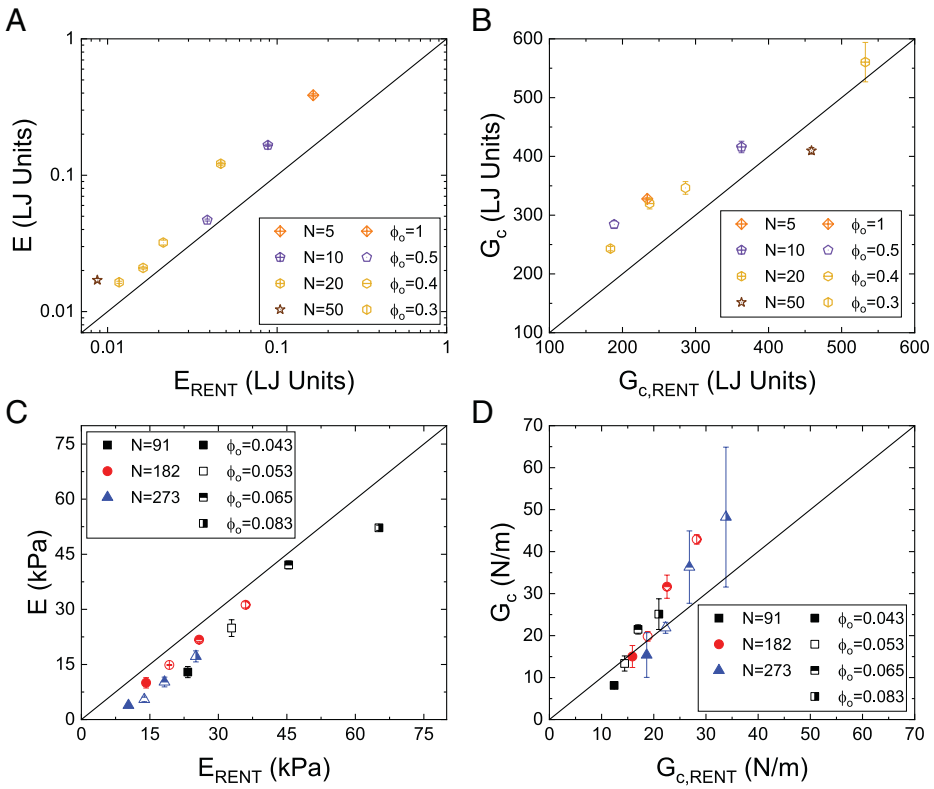

Fig. 4. Plots of E and G_c against E_{RENT} and $G_{c,RENT}$ measured during simulations (*A* and *B*) and with indentation and notch tests (*C* and *D*), described fully in *SI Appendix*, measured on a series of PEG gels in the as-prepared state (no additional swelling step). Simulation data are reported in reduced Lennard-Jones (LJ) units. Good agreement is observed between the measurements and the theory.

fracture plane and that this additional contribution can be accounted for by updating all of the terms in Lake–Thomas theory with an effective chain. The net effect of this correction results in a rescaling of the effective fracture plane height. Our model, while qualitatively similar, has several key differences from the models recently proposed by Arora et al. (34) and Lin and Zhao (51). First, Arora et al. (34) construct their model to include only contributions from real chains within the fracture plane, and they do not consider energy released in the neighboring network. Second, Arora et al. (34) empirically set their fracture plane height to be a constant value of 100 nm and then change the energy dissipated per chain and the chain density to account for loop defects. Importantly, Arora et al.'s (34) model predicts a reduction in fracture energy as the number of defects increases because these defects reduce the number of chains contained within the unadjusted fracture plane height. Lin and Zhao (51) argue that only the energy term, and not the fracture plane height or chain density, should be corrected, compared to our model that updates all of these terms. Notably, both our model and that of Lin and Zhao (51) predict an increase in the fracture energy with the introduction of loop defects. A comparison between the correction factor proposed in this work and those by Arora et al. (34) and Lin and Zhao (51) is shown in *SI Appendix*. Importantly, these differences have quantitative impact, allowing our model to describe experimental data without any fitting parameters.

Our theory proposes that the fracture plane should be defined by the effective size of the phantom chain (accounting for loop defects) instead of being limited to the physical size of a single chain as in classic Lake–Thomas theory. The loop correction decreases the estimate for E but increases the estimate for G_c. Both E and G_c suffer from a reduction in chain density; however, the increase in the size scale of dissipation offsets this reduction for G_c. As noted for elasticity theory, Eq. **7** collapses to a phantom network form of Lake–Thomas theory when $F_{eff} \to F$, which would occur at high values of $\nu {R_o}^3$. Plots of G_c against model predictions are shown in Fig. 4. The loop-modified Lake–Thomas theory displays good agreement with the fracture energies measured from experiments and simulations. This agreement shows that Lake–Thomas theory can be modified to account for loop defects in network structure.

While the model fits well for the PEG system where molecular parameters are known, it remains unclear how precisely these parameters must be known to accurately model fracture. A sensitivity analysis, presented in *SI Appendix*, shows that the loop-modified form of Lake–Thomas theory is most sensitive to errors in U where a 25% error in estimation leads to a 25% difference in model values.

Importantly, no fitting parameters or enhancement factors were used to produce the theoretical estimates of E and G_c. The strong agreement between theory and measurements presented above demonstrates that the fracture energy of polymer networks can be estimated from first principles by accounting for chain-level and network-level molecular structure when estimating U with the full bond dissociation energy.

Considering Local and Global Measurements of *U*

The results presented in the previous sections are predicated on the assumption that it is reasonable to estimate U using the full bond dissociation energy. This choice was justified using global calculations of the energy dissipated in the network during chain rupture; however, another test of this assumption would be to consider the local energy dissipated by each bond during chain rupture. These calculations have been performed and are described in detail in *SI Appendix*. We find that the ruptured bond, regardless of chain length, dissipates a quantity equivalent to the BDE, but the sum of the bond energies across N bonds

within a chain at the point of rupture is less than $N \times BDE$. At first glance, this finding appears to contradict the physical picture presented in Lake–Thomas theory, where the dissipated energy per chain is $N \times U$ (or $N \times BDE$). Upon further consideration, this finding provides insight into the relative contributions of bond energy and configurational entropy to the dissipated energy. The estimation of the average bond energy, which accounts only for the sum of bond energies per chain, neglects entropic contributions. These contributions have not been quantified in our current simulations, but the calculations of global energy dissipated per ruptured bond (Fig. 2*C*) suggest that N_{eff} closely accounts for these contributions. A first-principles understanding of how $N_{eff} \times U_{BDE}$ accounts for these contributions would provide more quantitative links between the single-chain (local) and network (global) dissipated energy values and BDE. Regardless, the correlation of our G_c values with the RENT-modified Lake–Thomas model, with no empirical fitting parameters, suggests an encouraging path for the next level of understanding network fracture.

Conclusions

The major finding of this paper is that the fracture properties of polymer networks can be predicted from molecular parameters without the need for empirical fitting parameters. This capability was demonstrated through carefully conducted experiments and simulations for model end-linked polymer networks. Insight with regard to the distribution of local and global contributions to the energy dissipated during network fracture was also gained. The simulations provide a means of comparing the dissipated energy during single-chain rupture and the global energy consumption in network fracture. This analysis demonstrates that the RENT-modified Lake–Thomas model describes the global energy consumed during network fracture and opens additional opportunities for understanding the entropic contributions of network fracture events. Overall, these results are anticipated to enable significant advances in materials design and use.

Materials and Methods

Materials and methods are described in detail in *SI Appendix*. This includes a description of the synthesis of the PEG gels employed in this work. The procedure used for swelling studies and measurement of the modulus of gels via indentation and pure shear tests is then described. The procedure for characterizing fracture energy of gels with pure shear notch tests is then described. Finally, the procedures used to estimate modulus and fracture energy of networks in the MD simulations are described. Summary data of the experiments are also provided in *SI Appendix*.

Data Availability. All study data are included in this article and/or *SI Appendix*.

ACKNOWLEDGMENTS. We acknowledge funding support from the Office of Naval Research (Grant N00014-17-1-2056). Computational resources were made available through Extreme Science and Engineering Discovery Environment Award TG-DMR150034. This work was supported in part by high performance computer time and resources from the Department of Defense High Performance Computing Modernization Program. We thank the reviewers for their careful consideration of the arguments used to estimate *U* in this article.

1. P. J. Flory, Network structure and the elastic properties of vulcanized rubber. *Chem. Rev.* **35**, 51–75 (1944).
2. F. T. Wall, Statistical thermodynamics of rubber. III. *J. Chem. Phys.* **11**, 527–530 (1943).
3. P. J. Flory, J. Rehner, Statistical mechanics of cross-linked polymer networks II. Swelling. *J. Chem. Phys.* **11**, 521–526 (1943).
4. L. Treloar, Stress–strain data for vulcanised rubber under various types of deformation. *Trans. Faraday Soc.* **39**, 59–70 (1943).
5. F. T. Wall, P. J. Flory, Statistical thermodynamics of rubber elasticity. *J. Chem. Phys.* **19**, 1435–1439 (1951).
6. L. R. Treloar, The photoelastic properties of short-chain molecular networks. *Trans. Faraday Soc.* **50**, 881–896 (1954).
7. C. G. Moore, W. F. Watson, Determination of degree of crosslinking in natural rubber vulcanizates. Part II. *J. Polym. Sci* **19**, 237–254 (1956).
8. L. Mullins, Determination of degree of crosslinking in natural rubber vulcanizates. Part III. *J. Appl. Polym. Sci.* **2**, 1–7 (1959).
9. S. Candau, A. Peters, J. Herz, Experimental evidence for trapped chain entanglements: Their influence on macroscopic behaviour of networks. *Polymer (Guildf.)* **22**, 1504–1510 (1981).
10. M. Rubinstein, S. Panyukov, Elasticity of polymer networks. *Macromolecules* **35**, 6670–6686 (2002).
11. M. Zhong, R. Wang, K. Kawamoto, B. D. Olsen, J. A. Johnson, Quantifying the impact of molecular defects on polymer network elasticity. *Science* **353**, 1264–1268 (2016).
12. P. E. Rouse, A theory of the linear viscoelastic properties of dilute solutions of coiling polymers. *J. Chem. Phys.* **21**, 1272–1280 (1953).
13. A. N. Semenov, M. Rubinstein, Thermoreversible gelation in solutions of associative polymers. 2. Linear dynamics. *Macromolecules* **31**, 1386–1397 (1998).
14. Y. Hu, X. Zhao, J. J. Vlassak, Z. Suo, Using indentation to characterize the poroelasticity of gels. *Appl. Phys. Lett.* **96**, 2008–2011 (2010).
15. J. Collis, D. L. Brown, M. E. Hubbard, R. D. O'Dea, Effective equations governing an active poroelastic medium. *Proc. Math. Phys. Eng. Sci.* **473**, 20160755 (2017).
16. Z. I. Kalcioglu, R. Mahmoodian, Y. Hu, Z. Suo, K. J. Van Vliet, From macro- to microscale poroelastic characterization of polymeric hydrogels via indentation. *Soft Matter* **8**, 3393–3398 (2012).
17. H. C. G. de Cagny *et al.*, Porosity governs normal stresses in polymer gels. *Phys. Rev. Lett.* **117**, 217802 (2016).
18. A. N. Gent, D. A. Tompkins, Nucleation and growth of gas bubbles in elastomers. *J. Appl. Phys.* **40**, 2520–2525 (1969).
19. A. N. Gent, J. Schultz, Effect of wetting liquids on the strength of adhesion of viscoelastic materials. *J. Adhes.* **3**, 281–294 (1972).
20. A. N. Gent, A new constitutive relation for rubber. *Rubber Chem. Technol.* **69**, 59–61 (1996).
21. P. G. de Gennes, Soft adhesives. *Langmuir* **12**, 4497–4500 (1996).
22. T. Baumberger, C. Caroli, D. Martina, Solvent control of crack dynamics in a reversible hydrogel. *Nat. Mater.* **5**, 552–555 (2006).
23. I. Naassaoui, O. Ronsin, T. Baumberger, A poroelastic signature of the dry/wet state of a crack tip propagating steadily in a physical hydrogel. *Extreme Mech. Lett.* **22**, 8–12 (2018).
24. F. Bueche, Molecular basis for the Mullins effect. *J. Appl. Polym. Sci.* **4**, 107–114 (1960).
25. J. Halpin, Molecular view of fracture in amorphous elastomers. *Rubber Chem. Technol.* **38**, 1007–1038 (1965).
26. G. J. Lake, A. G. Thomas, The strength of highly elastic materials. *Proc. R. Soc. Lond. A Math. Phys. Sci.* **300**, 108–119 (1967).
27. B. N. Persson, E. A. Brener, Crack propagation in viscoelastic solids. *Phys. Rev. E Stat. Nonlin. Soft Matter Phys.* **71** (3 Pt 2A), 036123 (2005).
28. A. Ahagon, A. N. Gent, Threshold fracture energies for elastomers. *J. Polym. Sci. Polym. Phys. Ed.* **13**, 1903–1911 (1975).
29. A. N. Gent, R. H. Tobias, Threshold tear strength of elastomers. *J. Polym. Sci. Polym. Phys. Ed.* **20**, 2051–2058 (1982).
30. T. Sakai *et al.*, Design and fabrication of a high-strength hydrogel with ideally homogeneous network structure from tetrahedron-like macromonomers. *Macromolecules* **41**, 5379–5384 (2008).
31. E. M. Saffer *et al.*, SANS study of highly resilient poly(ethylene glycol) hydrogels. *Soft Matter* **10**, 1905–1916 (2014).
32. S. Seiffert, Origin of nanostructural inhomogeneity in polymer-network gels. *Polym. Chem.* **3**, 4472–4487 (2017).
33. T. Sakai, Y. Akagi, S. Kondo, U. Chung, Experimental verification of fracture mechanism for polymer gels with controlled network structure. *Soft Matter* **10**, 6658–6665 (2014).
34. A. Arora *et al.*, Fracture of polymer networks containing topological defects. *Macromolecules* **53**, 7346–7355 (2020).
35. M. Malkoch *et al.*, Synthesis of well-defined hydrogel networks using click chemistry. *Chem. Commun. (Camb.)* **26**, 2774–2776 (2006).
36. J. Cui *et al.*, Synthetically simple, highly resilient hydrogels. *Biomacromolecules* **13**, 584–588 (2012).
37. H. Zhou *et al.*, Counting primary loops in polymer gels. *Proc. Natl. Acad. Sci. U.S.A.* **109**, 19119–19124 (2012).
38. B. D. Fairbanks *et al.*, A versatile synthetic extracellular matrix mimic via thiol-norbornene photopolymerization. *Adv. Mater.* **21**, 5005–5010 (2009).
39. J. Cui, M. A. Lackey, G. N. Tew, A. J. Crosby, Mechanical properties of end-linked PEG/PDMS hydrogels. *Macromolecules* **45**, 6104–6110 (2012).
40. K. Kawamoto, M. Zhong, R. Wang, B. D. Olsen, J. A. Johnson, Loops versus branch functionality in model click hydrogels. *Macromolecules* **48**, 8980–8988 (2015).
41. P. J. Flory, J. Rehner, Statistical mechanics of cross-linked polymer networks I. Rubberlike elasticity. *J. Chem. Phys.* **11**, 512–520 (1943).
42. H. B. Eitouni, N. P. Balsara, "Thermodynamics of polymer blends" in *Physical Properties of Polymers Handbook*, J. E. Mark, Ed. (Springer, New York, NY, 2006), pp. 339–356.
43. K. Kremer, G. S. Grest, Dynamics of entangled linear polymer melts: A molecular-dynamics simulation. *J. Chem. Phys.* **92**, 5057–5086 (1990).
44. T. Ge, F. Pierce, D. Perahia, G. S. Grest, M. O. Robbins, Molecular dynamics simulations of polymer welding: Strength from interfacial entanglements. *Phys. Rev. Lett.* **110**, 098301 (2013).
45. S. Wang, S. Panyukov, M. Rubinstein, S. L. Craig, Quantitative adjustment to the molecular energy parameter in the Lake-Thomas Theory of polymer fracture energy. *Macromolecules* **52**, 2772–2777 (2019).
46. D. J. Lacks, M. J. Osborne, Energy landscape picture of overaging and rejuvenation in a sheared glass. *Phys. Rev. Lett.* **93**, 255501 (2004).
47. H. N. Lee, R. A. Riggleman, J. J. de Pablo, M. Ediger, Deformation-induced mobility in polymer glasses during multistep creep experiments and simulations. *Macromolecules* **42**, 4328–4336 (2009).
48. S. Lin, J. Ni, D. Zheng, X. Zhao, Fracture and fatigue of ideal polymer networks. *Extreme Mech. Lett.* **48**, 101399 (2021).
49. P. Flory, Molecular theory of rubber elasticity. *Polymer (Guildf.)* **17**, 1–12 (1985).
50. H. M. James, Statistical properties of networks of flexible chains. *J. Chem. Phys.* **15**, 651–668 (1947).
51. S. Lin, X. Zhao, Fracture of polymer networks with diverse topological defects. *Phys. Rev. E* **102**, 052503 (2020).